Journal of Nuclear Medicine, published on September 9, 2021 as doi:10.2967/jnumed.121.262447

Pre-treatment sTNFR1 and HGF levels predict toxicity and overall survival after ^{90}Y radioembolization: potential novel application of biomarkers for personalized management of hepatotoxicity

Matthew M. Cousins[1†], Theresa P. Devasia[1†], Christopher M. Maurino[1], Justin Mikell[1], Matthew J. Schipper[1], Ravi K. Kaza[2], Theodore. S. Lawrence[1], Kyle C. Cuneo[1‖*], and Yuni K. Dewaraja[2‖]

[1]Department of Radiation Oncology, University of Michigan, Ann Arbor, MI, USA; [2]Department of Radiology, University of Michigan, Ann Arbor, MI, USA

***Corresponding author:** KCC, UH B2C490, 1500 E Medical Center Dr., Ann Arbor, MI 48109-5010, Phone: 734-936-4300, Fax: 734-763-7371, kcuneo@med.umich.edu

†Co-first author: MMC (resident, cousinma@med.umich.edu) and TPD (PhD student, tdevasia@umich.edu) contributed equally to this work. Other contact information per KCC.

‖Co-senior author: Authors contributed equally to this work.

Running title: Predictors of toxicity after ^{90}Y

Abstract

Liver function may be negatively affected by radiation for treatment of hepatic malignancy. Pretreatment blood cytokine levels are biomarkers for prediction of toxicity and survival after external beam radiation therapy. We hypothesized that cytokines may also predict outcomes after radioembolization, enabling a biomarker-driven personalized approach to treatment.

Methods: Pre-therapy blood samples from patients enrolled on a prospective protocol evaluating ^{90}Y radioembolization for management of intrahepatic malignancy were analyzed for two cytokines selected based on prior studies in stereotactic body radiotherapy (SBRT), soluble tumor necrosis factor receptor 1 (sTNFR1) and hepatocyte growth factor (HGF), via enzyme-linked immunosorbent assay (ELISA), and key dosimetric parameters were derived from post-treatment ^{90}Y PET/CT imaging. Toxicity was defined as a change in albumin-bilirubin score (ALBI) from baseline to follow up [3-6-month post-treatment (ΔALBI)]. Associations of cytokine levels, dose metrics, and baseline liver function with toxicity and overall survival were assessed.

Results: Data from 43 patients treated with ^{90}Y radioembolization for primary [48.8% (21/43)] or secondary [51.2% (22/43)] malignancy were assessed. Examined dose metrics and baseline liver function were not associated with liver toxicity; however, levels of sTNFR1 (p=0.045) and HGF (p=0.005) were associated with liver toxicity in univariate models. Cytokines were the only predictors of toxicity in multivariable models including dose metrics and prior liver directed therapy. sTNFR1 (HR 12.3; CI 3.5-42.5, p<0.001) and HGF (HR 7.5; CI 2.4-23.1, p<0.001) predicted overall survival, and findings were similar when models were controlled for absorbed dose and presence of metastatic disease. **Conclusions:** Pretreatment cytokine levels predict liver toxicity and overall survival. These pathways can be targeted with available drugs, an advantage over previously studied dose metrics and liver function tests. Interventions directed at the TNF alpha axis should be considered in future studies for prevention of liver toxicity, and HGF should be explored further to determine whether its elevation drives toxicity or indicates ongoing liver regeneration after prior injury.

Keywords: inflammation, cytokines, liver, toxicity

Introduction

Radioembolization with microspheres containing ^{90}Y is an established approach for treatment of malignancies involving the liver (*1*). A pretreatment 99mTc-macroaggregated albumin (MAA) scan is used to assess for enteric and pulmonary shunting prior to treatment with glass microspheres administered to achieve a dose to the targeted liver of 80-150 Gy (*2*). This approach currently relies on calculations that include perfused liver mass and pulmonary shunt fraction, but recent data suggest that the use of more personalized dosimetry can result in improved response rates with low rates of toxicity (*3-7*).

Side effects of radioembolization have been well-characterized and include lung toxicity, GI toxicity, and hepatotoxicity (*8*). Multiple studies have found that baseline liver function and dosimetry predict hepatotoxicity after radioembolization, suggesting that both should be considered for risk reduction (*6,7,9,10*). In contrast, our group and others have previously found that uninvolved liver absorbed dose is not correlated with toxicity (*11,12*). Though there remains some debate as to the importance of dose for toxicity prediction, it is important to consider other factors that show promise for prediction of liver toxicity following SBRT that might be applied to benefit patients receiving radioembolization.

Studies of liver toxicity after SBRT have shown that pretreatment levels of HGF and sTNFR1, predict hepatic injury after treatment (*13-15*). Additionally, baseline cytokine levels and inflammation-related lab values predict overall survival, suggesting even broader potential application of pretreatment lab-based studies (*14,16*). However, the linkage between these markers and overall survival has multiple potential explanations (e.g. relationships between markers and baseline liver status, risk of liver toxicity, local disease progression, systemic disease, and/or comorbid conditions). We have previously proposed that select cytokines portend an inflammatory state that could be targeted with the goal of reducing toxicity following radiation (*13*). Prior studies of hepatotoxicity and survival following radioembolization have focused on dose-metrics and liver function assessment, but some have considered blood

cytokine levels (*17-19*). To date, no study has simultaneously considered dose metrics, liver function, and biomarkers. We hypothesized that hepatotoxicity and overall survival after ^{90}Y radioembolization may be predicted by baseline cytokine levels and that these biomarkers might guide personalized treatment.

Materials and Methods

Study Population, Sample Collection, and Storage

Individuals with hepatic malignancy slated to receive treatment via ^{90}Y radioembolization (TheraSphere; BTG International Ltd.) at University of Michigan University Hospital (3/2017-2/2020) who met eligibility criteria (ability to undergo imaging, follow-up at the University of Michigan, and informed consent) were enrolled prospectively onto an Institutional Review Board-approved research study (UMCC 2016.090; HUM00118705) that included a blood draw and ^{90}Y PET/CT imaging. Participants provided written informed consent. Blood samples were collected before radioembolization; serum and plasma were prepared and stored (−80°C) until analysis, which was performed in 3/2020 in one batch after the last patient was enrolled.

Treatment

Prior to ^{90}Y treatment, each patient underwent an Tc-99m MAA scan to assess for shunting. The treating team adhered to standard guidelines for delivery of 80-150 Gy to the entirety of the treated liver lobe (40/43 lobar treatments; 3/43 selective treatments). Dose selection but not treatment strategy (selective vs lobar) depended upon disease histology, lung shunt, and baseline liver function. To achieve target doses, administered activities 0.5-12.6 GBq were delivered using microspheres with specific activity 107-1542 Bq/sphere.

Imaging and Segmentation

Post-treatment ^{90}Y PET/CT imaging reconstruction, registration, and segmentation was as described previously (*12*) and is summarized here. PET/CT imaging was performed within ~ 2 hours (average 2.5 h, range 1 – 5 h) of radioembolization with acquisition time ~30 min over a field encompassing the liver and portions of the thorax. Lesion contours segmented on pretreatment diagnostic CT or MRI by an experienced radiologist (RK) were transferred to ^{90}Y PET/CT following rigid registration (MIM Software, Cleveland, OH) with fine adjustment of location, guided by PET and CT, when mis-registration was evident. A total of 1-5 lesions >2 ml were segmented per patient. For the current study, liver segmentation was performed on CT of PET/CT using deep learning-based tools (MIM Software, Cleveland, OH). The liver volume minus the sum of segmented lesions (including a 1 cm expansion zone around each lesion to account for PET resolution) constituted the nontumoral liver volume that included the non-injected lobe. (Figure 1).

Dose variables

Voxel dosimetry was performed by coupling the quantitative ^{90}Y PET/CT images with explicit Monte Carlo radiation transport as described previously (*12*). Voxels within lesions and non-tumoral liver were scaled by volume-dependent recovery coefficients for a mean value partial volume correction (*12*). The following liver dose metrics were collected for the entire nontumoral liver volume: mean liver physical absorbed dose (MLD), mean liver biologically effective dose (BED; α/β=2.5 Gy; cell repair constant=0.28 h^{-1} (*6*)), mean liver biologically equivalent dose to radiation delivered at 2 Gy/fraction (EQD2), maximum dose to the coldest xx% (DCxx), and maximum dose to the coldest 700cc (DC700cc). DCxx and DC700cc were expressed as biologically effective dose for BEDCxx and BEDC700cc, respectively (*20*). As a surrogate for macroscopic non-uniformity, we calculated (DC10 – DC90)/DC50 and DC10 – DC90. Some patients received multiple treatments. When time between treatment was ≤90

days, dose values were generated using the summed PET/CT dose map from both treatments (Supplemental Figure 1). In this case, prior to summation the two dose maps were aligned based on a CT-CT rigid registration (MIM Software, Cleveland, OH) with manual fine-tuning. Summation of dosimetric data for treatments given ≤90 days apart was performed because it was felt that 90 days constitutes a first portion of the radiation response likely lasting at least 7 to 9 months as shown in the radiation induced liver injury literature and in studies of hypertrophy following radioembolization (*21,22*). Therefore, it is less likely that this 90-day period would be sufficient for significant recovery to occur prior to the second injury. Dose metrics from the first treatment were used if time between treatments was >90 days.

Toxicity assessment

Previous work has established ALBI score [$0.66 \times \log_{10}$Bilirubin (μmol/L) – $0.085 \times$ Albumin (g/L)] as a measure of liver function (*23*). The difference between ALBI score at baseline and a follow up assessment at 3-6 months was defined as ΔALBI. A positive ΔALBI is indicative of worsening liver function, considered the toxicity outcome in the current work. Additionally, relevant laboratory-based assessments were collected using Common Terminology Criteria for Adverse Events version 5 (CTCAE) within six months of treatment for alanine aminotransferase, aspartate aminotransferase, alkaline phosphatase, and total bilirubin.

Cytokine quantification

HGF (serum)and sTNFR1 (plasma) were quantified in appropriate specimens using Quantikine ELISA kits (R&D Systems, Minneapolis, MN): DRT100 (TNF-RI) and DHG00B (HGF). Assays were performed according to manufacturer recommendations without variation. Following assay development, absorbance data were collected and analyzed using a Synergy HT plate reader and Gen5 software, respectively (BioTek Instruments, Winooski, VT). Cytokine concentrations were determined through comparison to standards.

Statistical Methods

Correlations among the nontumoral liver dose metrics were measured using Pearson's correlation coefficient (ρ). Cytokine values were log transformed due to outliers. Univariate associations of ΔALBI and each of the dose metrics, HGF, and sTNFR1 were assessed using scatter plots. Based on the scatter plots, linear trends were identified. Univariate linear models with dose metrics, cytokines, or baseline disease factors were constructed. Multivariable models using the cytokines, dose metrics, and clinical factors were constructed. The association between cytokines and overall survival (OS) was assessed. Kaplan-Meier curves of OS stratified by median values of each cytokine were constructed and compared using the log-rank test. Univariate Cox proportional-hazards models were fit to quantify the effect of cytokines on risk of death. Harrell's c-index was used to quantify the predictive accuracy of survival models. Analyses were completed using R version 4.0.3.

RESULTS

Overview

Data were available from 43 patients with median age 65.0 years (Range: 37.0, 82.0) treated with ^{90}Y radioembolization for hepatocellular carcinoma [37.2% (16/43)], cholangiocarcinoma [11.6% (5/43)], or metastatic [51.2% (22/43)] malignancy (Table 1). Most patients [62.8% (27/43)] had a pre-treatment Child-Pugh score of 5. Toxicity outcome assessments included 34/43 (79.1%) patients with available ΔALBI. The median follow-up for toxicity was 6.0 months. Most patients [82.4% (28/34)] had positive ΔALBI, signifying worsening liver function. Six-month CTCAE grade toxicity data for liver-associated laboratory studies are provided in Supplemental Table 1. Median follow-up for survival was 10.9 months, and 25/43 of patients died during follow-up.

Absorbed dose and toxicity

Dose metrics are summarized in Table 1. Assessments included evaluation of relationships between dose metrics themselves and relationships between dose metrics and ΔALBI. Strong pairwise correlations were noted for MLD, BED, and EQD2 ($\rho>0.8$, Supplemental Table 2). BEDC10, BEDC30, BEDC90, and BEDC700cc were also strongly correlated with DC10, DC30, DC90, and DC700cc, respectively ($\rho>0.96$, Supplemental Table 2). Simple linear fits demonstrated greatest positive associations between three dose metrics in particular (MLD, DC700cc, and DC90) and ΔALBI (Supplemental Figure 2); however, none of these associations were statistically significant (Table 2). Only MLD and DC90 were selected for multivariable modeling because 1) strong relationships were noted between dose metrics and 2) the identification of a subset of metrics, including MLD and DC90, with the strongest associations with ΔALBI. The effect of dose heterogeneity on toxicity was also examined, and neither of two measures of dose uniformity that we evaluated, (DC10 – DC90)/DC50 or DC10 – DC90, were associated with toxicity (Table 2).

Cytokines and toxicity

Higher baseline levels of sTNFR1 and HGF were associated with a larger ΔALBI (Fig. 2A, 2B). Formal models were constructed to characterize relationships between cytokine levels at baseline and toxicity as measured by ΔALBI. Baseline HGF ($p=0.005$) and sTNFR1 ($p=0.045$) were significantly associated with greater liver toxicity (Table 2). Metastatic disease, baseline ALBI score, baseline cirrhosis, number of prior liver-directed therapies, and number of prior systemic therapies were not significantly associated with toxicity.

After discovering that a subset of the selected cytokines predicted toxicity, multivariable toxicity models incorporating select dose metrics, cytokines, and clinical covariates were constructed (Table 3). When models were adjusted for baseline ALBI score, receipt of prior liver-directed therapy, and either MLD or DC90, HGF ($p<0.002$) and sTNFR1 ($p<0.030$) were

significant predictors of toxicity. Models with DC700cc demonstrated similar findings (Supplemental Table 3). Relationships among cytokines were assessed to determine if they provide independent information. Baseline HGF and sTNFR1 were positively correlated (ρ=0.50, Supplemental Table 4); when a multivariable toxicity model including all three cytokines was constructed, only HGF was significant (Supplemental Table 5).

Cytokines and overall survival

After determining that cytokine levels were associated with toxicity, we examined cytokines for prediction of overall survival. Baseline sTNFR1 (p=0.010; Fig. 3A) and HGF (p=0.011; Fig. 3B) above the median for each cytokine were associated with worse survival. Median OS was 33.3 months (95% CI [10.9, NA]) and 10.9 months (95% CI [5.9, NA]) for those with baseline sTNFR1 concentration below vs. above the median, respectively (Table 4). Median OS was 33.3 months (95% CI [10.9, NA]) and 9.8 months (95% CI [6.4, NA]) for those with baseline HGF concentrations below vs. above the median, respectively (Table 4).

Continuous models found that elevated levels of sTNFR1 (HR 12.3, p<0.001, c-index=0.71) and HGF (HR 7.5, p<0.001, c-index=0.69) were significantly associated with increased risk of death (Table 5). No dose metrics predicted survival (Supplemental Table 6). In multivariable models adjusting for DC90 or MLD and metastatic disease, sTNFR1 and HGF were strong predictors of survival (p<0.001).

Discussion

In the current study, we show that baseline elevations in HGF and sTNFR1 levels predict liver toxicity and overall survival after ^{90}Y radioembolization for management of hepatic malignancy, validating our previous findings in setting of SBRT (*13,14*). Levels of these soluble signaling molecules appear to be more important for prediction of toxicity than radiation dose and even baseline liver function in patients with both primary and secondary hepatic

malignancy. With additional studies, these biomarkers could be used to guide patient care in the pretreatment setting by providing valuable prognostic information regarding both toxicity and overall survival. As signaling through both entities is targetable, our findings support future trials of interventions in the pretreatment setting for prevention of hepatotoxicity after radioembolization.

Many have implicated TNFα as a potential mediator of inflammatory signals that result in liver injury (*24,25*). TNFR1 is a ubiquitously expressed plasma membrane-associated molecule that transduces extracellular signals into the intracellular environment (*26*). The soluble form of TNFR1 (sTNFR1) is released constitutively, but sTNFR1 shedding increases with exposure to TNFα (*27-29*). Elevated sTNFR1 levels are associated with liver inflammation (*30*). Two key preclinical studies linked radiation to liver injury mediated by the TNFα axis. First, when hepatocytes were irradiated in the presence of TNFα, higher levels of apoptotic cell death were observed (*31*). Second, hepatocyte apoptosis was prevented in irradiated cells when they were treated with antisense oligonucleotides against TNFR1 in the presence of TNFα (*32*). Therefore, sTNFR1 represents a stable analyte for assessment of TNFα signaling that has previously been linked to liver toxicity after SBRT (*13*) and for the first time has been linked to liver toxicity following ^{90}Y radioembolization in the current study.

HGF was also predictive of liver toxicity following SBRT, as previously shown by our group and others (*14,15*). The mechanism through which one might explain these relationships is less clear. c-MET, the major downstream signaling target of HGF, is a receptor tyrosine kinase (*33*), and HGF signaling through this molecule is mitogenic, driving regeneration after liver injury or resection (*34-36*). However, there is some disagreement in the literature as to whether c-Met promotes hepatocyte recovery or fibrosis (*37,38*). HGF-MET signaling has also been linked to unfavorable tumor characteristics, including metastasis and invasion (*33*).

Our finding that sTNFR1 and HGF predicted liver toxicity following ^{90}Y radioembolization presents multiple potential opportunities for personalized medicine. FDA-approved small

molecule inhibitors targeting the TNFα axis and c-Met, the signaling partner of HGF (*39,40*), should be considered in future clinical trials for prevention of toxicity. The fact that these signaling entities (sTNFR1 and HGF) might be targeted for potential therapeutic gain constitutes a major advantage over biomarkers or scores that can only direct treatment adaptation or avoidance. However, further study of HGF is needed prior to targeting this entity to ensure that HGF is driving toxicity and not simply elevated in setting of liver recovery (*18*).

The impact of dose on liver toxicity after radioembolization has been widely discussed in the ^{90}Y literature (*6*). We did not note associations between dose and toxicity, though others have shown the presence (*10*) and absence (*11,12*) of such relationships. One explanation for this difference is that our sample included a nearly even mixture of those with primary and secondary malignancy with generally good liver function. Additionally, our sample size was small. Despite our findings, we encourage continued efforts toward more personalized dosimetry to balance disease control and toxicity given positive results in recent studies (*5,9*).

Relationships between signaling molecules and overall survival are more difficult to explain than the toxicity relationships reviewed above. It is important to consider non-liver and/or non-oncologic disease states along with liver disease, cancer status, and treatment toxicity as potential explanations for both increases in cytokines and worse survival. Regardless of the potential mechanistic explanations, these relationships are significant and should be evaluated in future studies with the goal of applying their prognostic power to guide clinical decision-making.

There are several weaknesses of this work that we would like to note. The study is relatively small and was conducted at a single institution, suggesting that analyses may have been underpowered and that a limited number of treatment scenarios might have been captured. Though care was taken in registration of images and segmentation, it is not possible to eliminate the impact of misregistration on dosimetric calculations. The impact of misregistration and the use of rigid registration for dose accumulation are limitations of the

study. Though beyond the scope of this study, additional studies are needed to determine the value of deformable registration for Y90 and if changes in technique (e.g. higher exposure, use of contrast) of the CT of PET/CT are necessary to yield accurate deformable maps from a diagnostic quality scan to CT of PET/CT that is performed without contrast and with low mAs. Respiratory motion effects might also impact dosimetric calculations, though mean nontumoral liver dose, which is the dose metric we focus on in the current paper, has been shown to be insensitive to respiratory motion up to 4 cm in a simple phantom study (*41*). Furthermore, although we evaluated macroscale level heterogeneity indices, the impact of dose deposition non-uniformity at the microscale level (*42,43*) was not evaluated due to the challenges of doing this with resolution capabilities of PET. Despite these limitations, this study validates prior work in SBRT demonstrating the importance of cytokines for toxicity prediction after liver irradiation. When combined with prior work demonstrating relationships between disease response and ^{90}Y PET dosimetry (*12*), the findings of the current study hold great promise for personalized treatment planning. This study will inform larger clinical studies in the SBRT and radioembolization spaces to select and validate biomarker cut points to facilitate their use in patient selection and to test approaches to directly target processes driving liver damage in those at higher risk for toxicity.

Conclusions

HGF and sTNFR1 levels prior to ^{90}Y radioembolization predict both post-treatment hepatotoxicity and overall survival. These findings support larger studies to identify cutoffs for signaling molecules, a clinical trial of TNF axis inhibitors for prevention of liver toxicity, and further preclinical examination of the relationship between HGF and liver toxicity. These data will facilitate the development of novel biomarker-based approaches for prediction and intervention to address hepatotoxicity after radioembolization, an improvement over using only dosimetry and liver function assessments that have been the focus of hepatotoxicity prevention efforts to date.

DISCLOSURE: No relevant conflict of interest is reported. This work was supported by the National Institutes of Health [1R01EB022075 to YKD] and University of Michigan Comprehensive Cancer Center Support Grant (Project#:3P30CA046592).

ACKNOWLEDGEMENTS: The authors would like to thank Joel Whitfield for assistance with cytokine quantification.

Key Points

QUESTION: Do baseline cytokine levels predict liver toxicity and/or overall survival in those treated with ^{90}Y radioembolization for hepatic malignancy to enable a novel biomarker driven personalized approach to treatment?

PERTINENT FINDINGS: Pretreatment HGF and sTNFR1 levels predicted liver toxicity and overall survival, while ^{90}Y PET/CT-derived absorbed dose metrics did not.

IMPLICATIONS FOR PATIENT CARE: With further study and validation, HGF and/or sTNFR1 might be used for pretreatment patient stratification or treatment adaptation to avoid toxicity. Interventional trials of TNFα axis modifying agents and c-MET inhibitors should be considered.

References

1. Salem R, Gabr A, Riaz A, et al. Institutional decision to adopt Y90 as primary treatment for hepatocellular carcinoma informed by a 1,000-patient 15-year experience. *Hepatology.* 2018;68:1429-1440.

2. BTG[package-insert]. *TheraSphere® Yttrium-90 Glass Microspheres* Undated.

3. Salem R, Padia SA, Lam M, et al. Clinical and dosimetric considerations for Y90: recommendations from an international multidisciplinary working group. *Eur J Nucl Med Mol Imaging.* 2019;46:1695-1704.

4. Strigari L, Sciuto R, Rea S, et al. Efficacy and Toxicity Related to Treatment of Hepatocellular Carcinoma with ⁹⁰Y-SIR Spheres: Radiobiologic Considerations. *Journal of Nuclear Medicine.* 2010;51:1377-1385.

5. Garin E, Tselikas L, Guiu B, et al. Personalised versus standard dosimetry approach of selective internal radiation therapy in patients with locally advanced hepatocellular carcinoma (DOSISPHERE-01): a randomised, multicentre, open-label phase 2 trial. *Lancet Gastroenterol Hepatol.* 2021;6:17-29.

6. Cremonesi M, Chiesa C, Strigari L, et al. Radioembolization of hepatic lesions from a radiobiology and dosimetric perspective. *Front Oncol.* 2014;4:210.

7. Chiesa C, Mira M, Maccauro M, et al. Radioembolization of hepatocarcinoma with (90)Y glass microspheres: development of an individualized treatment planning strategy based on dosimetry and radiobiology. *Eur J Nucl Med Mol Imaging.* 2015;42:1718-1738.

8. Riaz A, Awais R, Salem R. Side effects of yttrium-90 radioembolization. *Front Oncol.* 2014;4:198.

9. Garin E, Palard X, Rolland Y. Personalised Dosimetry in Radioembolisation for HCC: Impact on Clinical Outcome and on Trial Design. *Cancers (Basel).* 2020;12:1557.

10. Chiesa C, Mira M, Bhoori S, et al. Radioembolization of hepatocarcinoma with (90)Y glass microspheres: treatment optimization using the dose-toxicity relationship. *Eur J Nucl Med Mol Imaging.* 2020;47:3018-3032.

11. Kappadath SC, Mikell J, Balagopal A, Baladandayuthapani V, Kaseb A, Mahvash A. Hepatocellular Carcinoma Tumor Dose Response After (90)Y-radioembolization With Glass Microspheres Using (90)Y-SPECT/CT-Based Voxel Dosimetry. *Int J Radiat Oncol Biol Phys.* 2018;102:451-461.

12. Dewaraja YK, Devasia T, Kaza RK, et al. Prediction of Tumor Control in (90)Y Radioembolization by Logit Models with PET/CT-Based Dose Metrics. *J Nucl Med.* 2020;61:104-111.

13. Cousins MM, Morris E, Maurino C, et al. TNFR1 and the TNFα axis as a targetable mediator of liver injury from stereotactic body radiation therapy. *Transl Oncol.* 2021;14:100950.

14. Cuneo KC, Devasia T, Sun Y, et al. Serum Levels of Hepatocyte Growth Factor and CD40 Ligand Predict Radiation-Induced Liver Injury. *Transl Oncol.* 2019;12:889-894.

15. Hong TS, Grassberger C, Yeap BY, et al. Pretreatment plasma HGF as potential biomarker for susceptibility to radiation-induced liver dysfunction after radiotherapy. *NPJ Precis Oncol.* 2018;2:22.

16. Lo C-H, Lee H-L, Hsiang C-W, et al. Pretreatment Neutrophil-to-Lymphocyte Ratio Predicts Survival and Liver Toxicity in Patients With Hepatocellular Carcinoma Treated With Stereotactic Ablative Radiation Therapy. *International Journal of Radiation Oncology, Biology, Physics.* 2021;109:474-484.

17. Seidensticker M, Powerski M, Seidensticker R, et al. Cytokines and 90Y-Radioembolization: Relation to Liver Function and Overall Survival. *CardioVascular and Interventional Radiology.* 2017;40:1185-1195.

18. Fernandez-Ros N, Iñarrairaegui M, Paramo JA, et al. Radioembolization of hepatocellular carcinoma activates liver regeneration, induces inflammation and endothelial stress and activates coagulation. *Liver International.* 2015;35:1590-1596.

19. Wickremesekera JK, Chen W, Cannan RJ, Stubbs RS. Serum proinflammatory cytokine response in patients with advanced liver tumors following selective internal radiation therapy (SIRT) with 90Yttrium microspheres. *International Journal of Radiation Oncology*Biology*Physics.* 2001;49:1015-1021.

20. Miften M, Vinogradskiy Y, Moiseenko V, et al. Radiation Dose-Volume Effects for Liver SBRT. *Int J Radiat Oncol Biol Phys.* 2018;110:196-205.

21. Teo JY, Allen JC, Jr., Ng DC, et al. A systematic review of contralateral liver lobe hypertrophy after unilobar selective internal radiation therapy with Y90. *HPB (Oxford).* 2016;18:7-12.

22. Lawrence TS, Robertson JM, Anscher MS, Jirtle RL, Ensminger WD, Fajardo LF. Hepatic toxicity resulting from cancer treatment. *Int J Radiat Oncol Biol Phys.* 1995;31:1237-1248.

23. Johnson PJ, Berhane S, Kagebayashi C, et al. Assessment of liver function in patients with hepatocellular carcinoma: a new evidence-based approach-the ALBI grade. *J Clin Oncol.* 2015;33:550-558.

24. Kusters S, Tiegs G, Alexopoulou L, et al. In vivo evidence for a functional role of both tumor necrosis factor (TNF) receptors and transmembrane TNF in experimental hepatitis. *Eur J Immunol.* 1997;27:2870-2875.

25. Yang YM, Seki E. TNFα in liver fibrosis. *Current pathobiology reports.* 2015;3:253-261.

26. Holbrook J, Lara-Reyna S, Jarosz-Griffiths H, McDermott M. Tumour necrosis factor signalling in health and disease. *F1000Res.* 2019;8.

27. Aderka D, Sorkine P, Abu-Abid S, et al. Shedding kinetics of soluble tumor necrosis factor (TNF) receptors after systemic TNF leaking during isolated limb perfusion. Relevance to the pathophysiology of septic shock. *J Clin Invest.* 1998;101:650-659.

28. Pinckard JK, Sheehan KC, Arthur CD, Schreiber RD. Constitutive shedding of both p55 and p75 murine TNF receptors in vivo. *J Immunol.* 1997;158:3869-3873.

29. Xia M, Xue SB, Xu CS. Shedding of TNFR1 in regenerative liver can be induced with TNF alpha and PMA. *World J Gastroenterol.* 2002;8:1129-1133.

30. Abiru S, Migita K, Maeda Y, et al. Serum cytokine and soluble cytokine receptor levels in patients with non-alcoholic steatohepatitis. *Liver Int.* 2006;26:39-45.

31. Christiansen H, Saile B, Neubauer-Saile K, et al. Irradiation leads to susceptibility of hepatocytes to TNF-alpha mediated apoptosis. *Radiother Oncol.* 2004;72:291-296.

32. Huang XW, Yang J, Dragovic AF, Zhang H, Lawrence TS, Zhang M. Antisense oligonucleotide inhibition of tumor necrosis factor receptor 1 protects the liver from radiation-induced apoptosis. *Clin Cancer Res.* 2006;12:2849-2855.

33. Gherardi E, Birchmeier W, Birchmeier C, Vande Woude G. Targeting MET in cancer: rationale and progress. *Nat Rev Cancer.* 2012;12:89-103.

34. Matsumoto K, Nakamura T. Hepatocyte growth factor: molecular structure, roles in liver regeneration, and other biological functions. *Crit Rev Oncog.* 1992;3:27-54.

35. Efimova EA, Glanemann M, Nussler AK, et al. Changes in serum levels of growth factors in healthy individuals after living related liver donation. *Transplant Proc.* 2005;37:1074-1075.

36. Ishiki Y, Ohnishi H, Muto Y, Matsumoto K, Nakamura T. Direct evidence that hepatocyte growth factor is a hepatotrophic factor for liver regeneration and has a potent antihepatitis effect in vivo. *Hepatology.* 1992;16:1227-1235.

37. Giebeler A, Boekschoten MV, Klein C, et al. c-Met confers protection against chronic liver tissue damage and fibrosis progression after bile duct ligation in mice. *Gastroenterology.* 2009;137:297-308, 308.e291-294.

38. Krawczyk M, Zimmermann S, Hess G, et al. Panel of three novel serum markers predicts liver stiffness and fibrosis stages in patients with chronic liver disease. *PLOS ONE.* 2017;12:e0173506.

39. Puccini A, Marín-Ramos NI, Bergamo F, et al. Safety and Tolerability of c-MET Inhibitors in Cancer. *Drug safety.* 2019;42:211-233.

40. Chiang GT, Glaser RL. Clinical Review: GP2015 (proposed biosimilar to US-licensed Enbrel). FDA: https://www.fda.gov/media/105952/download; 2016.

41. Siman W, Mawlawi OR, Mikell JK, Mourtada F, Kappadath SC. Effects of image noise, respiratory motion, and motion compensation on 3D activity quantification in count-limited PET images. *Phys Med Biol.* 2017;62:448-464.

42. Pasciak AS, Abiola G, Liddell RP, et al. The number of microspheres in Y90 radioembolization directly affects normal tissue radiation exposure. *European Journal of Nuclear Medicine and Molecular Imaging.* 2020;47:816-827.

43. d'Abadie P, Hesse M, Jamar F, Lhommel R, Walrand S. (90)Y TOF-PET based EUD reunifies patient survival prediction in resin and glass microspheres radioembolization of HCC tumours. *Phys Med Biol.* 2018;63:245010.

TABLES

Table 1. Summary of patient characteristics, radiation dose, and outcomes. Continuous factors summarized as Median [Min, Max] and categorical factors summarized as # (%).

Variable	Summary
N	43
Age at ^{90}Y (years)	65.0 [37.0, 82.0]
Female gender	17 (39.5)
White race	38 (88.4)
Baseline cirrhosis	16 (37.2)
Cancer details	–
Primary	21 (48.8)
HCC	16 (37.2)
Metastatic	22 (51.2)
Treatment history	–
Prior liver-directed therapy	15 (34.9)
Prior systemic therapy	26 (60.0)
Two ^{90}Y treatments	14 (32.6)
Baseline liver scores	–
Child-Pugh	–
5	27 (62.8)
6	11 (25.6)
7	1 (2.3)
8	N/A
9	1 (2.3)
Unavailable	3 (7.0)
MELD-NA	9.0 [6.4, 18.7]
Baseline ALBI	-2.70 [-3.38, -1.28]
Dose metrics (Gy)	–
Mean Dose	50.2 [1.2, 132.1]
Mean BED	145.1 [1.3, 770.5]
DC10	0.9 [0.0, 40.0]
DC90	128.7 [1.7, 345.1]
DC700cc	15.7 [0.2, 203.1]
Baseline cytokines (pg/mL)	–
sTNFR1	1736.5 [924.4, 5518.0]
HGF	2557.7 [1328.1, 6876.2]
Outcomes	–
Toxicity follow-up (months)	6.0 [3.0, 6.0]
ΔALBI (n=34)	0.3 [-0.3, 1.9]
Positive ΔALBI (n=34)	28 (82.4)
Overall survival follow-up (months)	10.9 [1.2, 41.8]
Number deaths	25 (58.1)

Table 2. Univariate linear models for ΔALBI.

Model	Covariate	Coefficient	R^2	95% CI LB	95% CI UB	p-value
1	MLD	0.001	0.004	-0.004	0.006	0.737
2	BED	0.000	0.0001	-0.001	0.001	0.951
3	DC10	0.001	0.0002	-0.017	0.018	0.940
4	DC30	-0.001	0.001	-0.009	0.007	0.866
5	DC90	0.001	0.028	-0.001	0.003	0.348
6	DC700cc	0.001	0.004	-0.002	0.003	0.734
7	DC10-DC90	-0.001	0.029	-0.003	0.001	0.333
8	(DC10-DC90)/DC50	0.001	0.013	-0.002	0.005	0.524
9	Log(sTNFR1)	0.477	0.119	0.029	0.925	0.045
10	Log(HGF)	0.572	0.222	0.201	0.944	0.005
11	# Pre-^{90}Y Liver Therapies	-0.020	0.002	-0.171	0.130	0.792
12	Cirrhosis	0.195	0.044	-0.122	0.513	0.236
13	Metastatic	-0.082	0.008	-0.400	0.236	0.615
14	Baseline ALBI Score	0.014	0.0001	-0.385	0.413	0.947
15	Baseline Child-Pugh = 6	0.077	0.005	-0.307	0.462	0.696
	Baseline Child-Pugh = 7	-0.006		-0.968	0.956	0.990
16	# Pre-^{90}Y Systemic Therapies	-0.087	0.042	-0.232	0.058	0.247

Table 3. Multivariable linear models for ΔALBI.

Model	Covariate	Coefficient	95% CI LB	95% CI UB	p-value
1	MLD	0.003	-0.002	0.008	0.319
	Log(sTNFR1)	0.622	0.099	1.145	0.027
	Baseline ALBI Score	-0.166	-0.583	0.251	0.442
	Prior Liver Directed Therapy	-0.026	-0.362	0.311	0.883
2	MLD	0.003	-0.001	0.008	0.181
	Log(HGF)	0.709	0.285	1.133	0.003
	Baseline ALBI Score	-0.143	-0.514	0.229	0.458
	Prior Liver Directed Therapy	0.079	-0.246	0.405	0.636
3	DC90	0.002	-0.0004	0.004	0.124
	Log(sTNFR1)	0.628	0.132	1.125	0.019
	Baseline ALBI Score	-0.081	-0.493	0.331	0.702
	Prior Liver Directed Therapy	-0.034	-0.359	0.290	0.837
4	DC90	0.002	-0.00003	0.004	0.064
	Log(HGF)	0.706	0.306	1.106	0.002
	Baseline ALBI Score	-0.045	-0.414	0.324	0.813
	Prior Liver Directed Therapy	0.065	-0.245	0.375	0.686

Table 4. Median OS estimates in months, 95% CI, and number (%) deaths by median values of each cytokine.

Cytokine	Median OS (months)	95% CI LB	95% CI UB	# Deaths	% Deaths
sTNFR1 ≤ Median	33.3	10.9	NA	10	45.5
sTNFR1 > Median	10.9	5.9	NA	15	71.4
HGF ≤ Median	33.3	10.9	NA	9	40.9
HGF > Median	9.8	6.4	NA	16	76.2

Table 5. Univariate and multivariable Cox proportional-hazards model results for OS.

Model	Covariate	HR	95% CI LB	95% CI UB	p-value	c-index
1	Log(sTNFR1)	12.27	3.54	42.53	<0.001	0.71
2	Log(HGF)	7.48	2.42	23.08	<0.001	0.69
3	MLD (Gy)	0.99	0.98	1.01	0.403	0.58
4	DC90 (Gy)	0.99	0.99	1.00	0.383	0.55
5	Log(sTNFR)	18.76	4.95	71.14	<0.001	0.71
	Metastatic	2.27	0.87	5.93	0.093	
	DC90 (Gy)	0.99	0.99	1.00	0.521	
6	Log(HGF)	15.32	3.93	59.74	<0.001	0.72
	Metastatic	2.98	1.01	8.81	0.049	
	DC90 (Gy)	0.99	0.99	1.00	0.516	
7	Log(sTNFR)	19.32	5.12	72.86	<0.001	0.70
	Metastatic	2.36	0.92	6.05	0.075	
	MLD (Gy)	0.99	0.98	1.01	0.348	
8	Log(HGF)	15.60	4.05	60.14	<0.001	0.72
	Metastatic	3.22	1.05	9.90	0.042	
	MLD (Gy)	0.99	0.98	1.01	0.426	

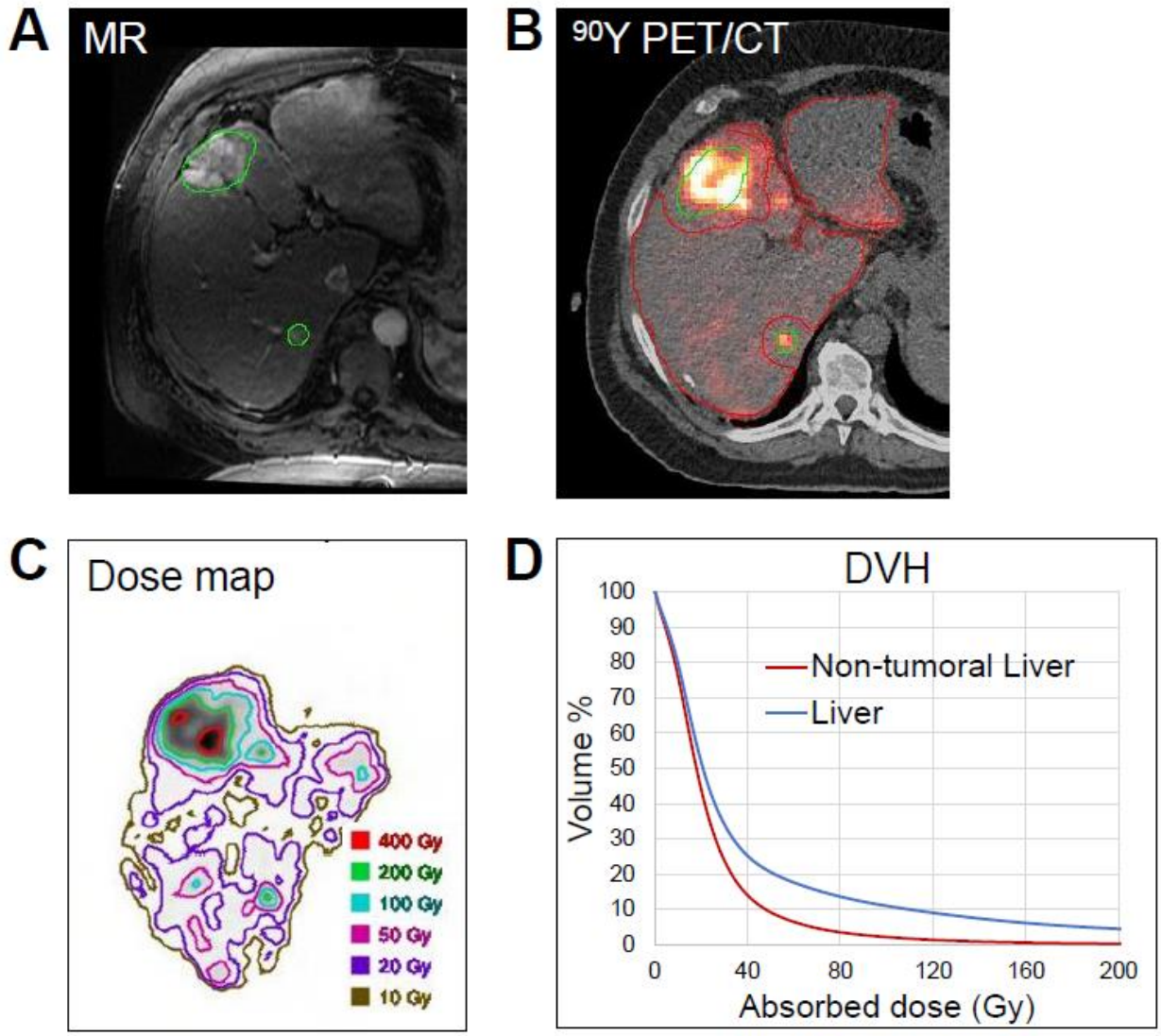

Figure 1. Example (A) baseline MR and (B) ^{90}Y PET/CT following treatment (3.2 GBq) are shown. Lesion contours (green) defined on MR and applied to co-registered PET/CT. Non-tumoral liver (red) accounts for 1 cm expansion around lesions to address PET resolution. (C) dose map and (D) DVH are provided for treatment with MLD 24 Gy and DC90 48 Gy.

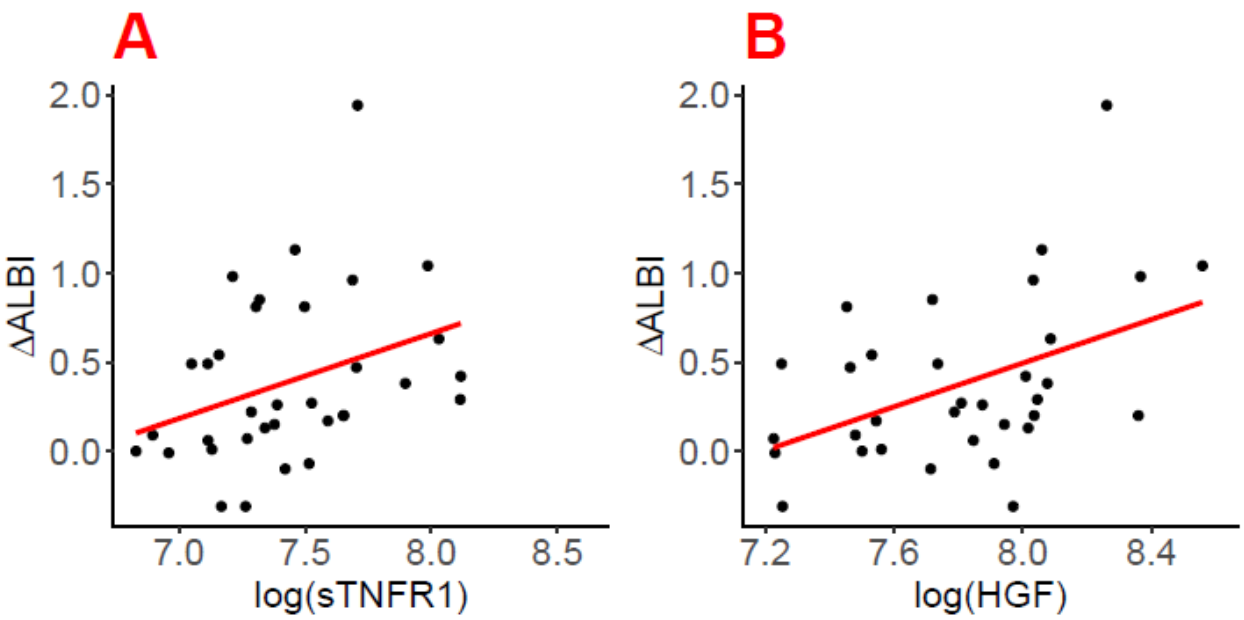

Figure 2. Scatterplots of log-transformed (A) sTNFR1 and (B) HGF vs. ΔALBI. Solid red line represents simple linear fit.

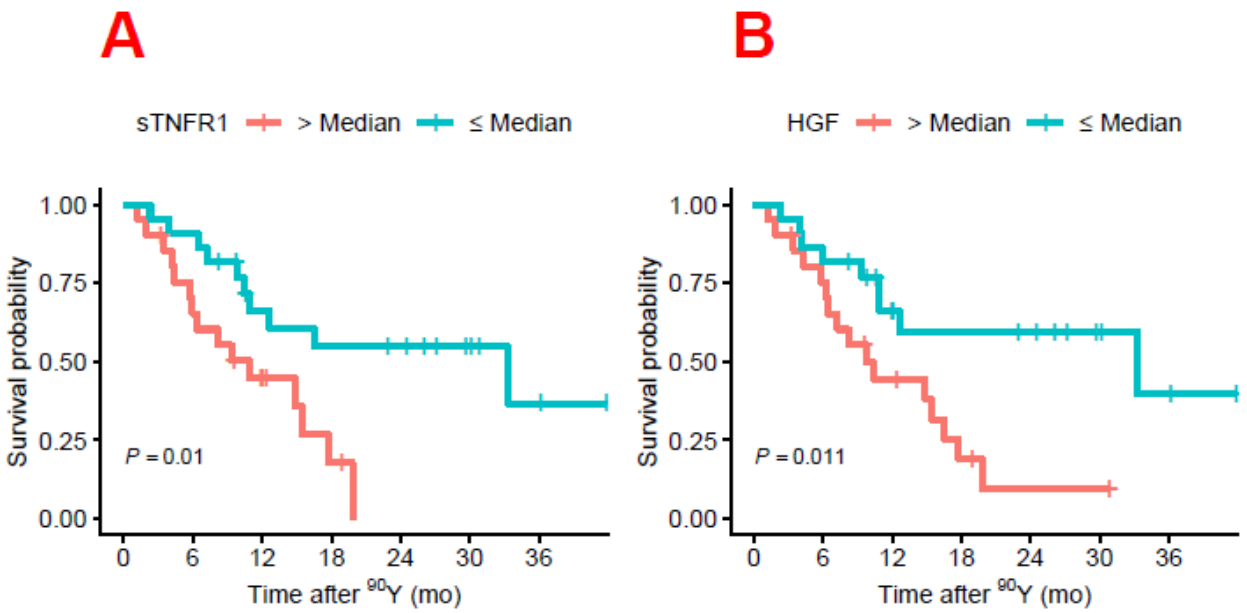

Figure 3. Kaplan-Meier curves for OS stratified by median value of (A) sTNFR1 and (B) HGF with log-rank p-value.

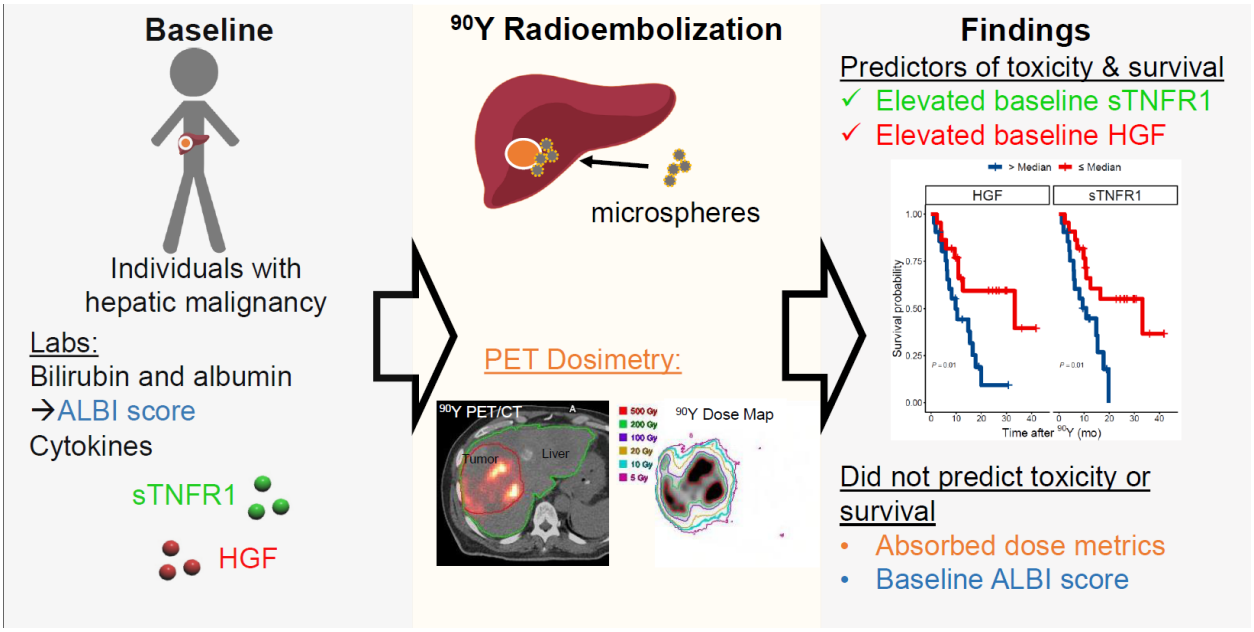

Graphical Abstract

Supplementary Appendix

Title: Impact of dose, clinical factors, and pre-treatment cytokine levels on toxicity after ^{90}Y radioembolization for hepatic malignancy

Authors: Matthew M. Cousins[a†], Theresa P. Devasia[a†], Christopher M. Maurino[a], David Karnak[a], Justin Mikell[a], Matthew J. Schipper[a], Ravi K. Kaza[b], Theodore. S. Lawrence[a], Kyle C. Cuneo[a‖*], and Yuni K Dewaraja[b‖]

Affiliations: [a]Department of Radiation Oncology, University of Michigan, UH B2C490, 1500 E Medical Center Dr, Ann Arbor, MI 48109-5010, USA; [b]Department of Radiology, University of Michigan, MI, USA

[†]Co-first author: These authors contributed equally to this work.
[‖]Co-senior author: These authors contributed equally to this work.
*Corresponding Author

Note: p-values highlighted in red on the following pages are significant at 0.05 level.

Supplemental Table 1. Six-month CTCAE liver toxicity grade outcomes for 34 patients with measures available at six months per CTCAE v5.0.

CTCAE Grade	AST	ALT	Alkphos	Total Bilirubin
0	10	16	11	22
1	17	16	18	3
2	5	1	3	6
3	1	N/A	2	3
4	1	1	N/A	N/A
Total	34	34	34	34

Supplemental Table 2. Correlation (ρ) matrix for healthy liver dose metrics among 43 patients with measured cytokines and uncensored for systemic focal therapy. All doses are measured in Gy.

	MLD	BED	EQD2	DC10	DC30	DC90	DC700cc	BEDC10	BEDC30	BEDC90	BEDC700cc
MLD	1.00	0.83	0.83	0.69	0.80	0.83	0.75	0.67	0.76	0.75	0.68
BED	0.83	1.00	1.00	0.39	0.49	0.73	0.58	0.37	0.45	0.72	0.53
EQD2	0.83	1.00	1.00	0.39	0.49	0.73	0.58	0.37	0.45	0.72	0.53
DC10	0.69	0.39	0.39	1.00	0.96	0.33	0.55	1.00	0.97	0.27	0.47
DC30	0.80	0.49	0.49	0.96	1.00	0.41	0.63	0.95	0.99	0.34	0.55
DC90	0.83	0.73	0.73	0.33	0.41	1.00	0.56	0.32	0.38	0.97	0.53
DC700cc	0.75	0.58	0.58	0.55	0.63	0.56	1.00	0.54	0.61	0.55	0.97
BEDC10	0.67	0.37	0.37	1.00	0.95	0.32	0.54	1.00	0.97	0.26	0.46
BEDC30	0.76	0.45	0.45	0.97	0.99	0.38	0.61	0.97	1.00	0.32	0.54
BEDC90	0.75	0.72	0.72	0.27	0.34	0.97	50.55	0.26	0.32	1.00	0.52
BEDC700cc	0.68	0.53	0.53	0.47	0.55	0.53	0.97	0.46	0.54	0.52	1.00

Supplemental Table 3. Multivariable linear models for ΔALBI with cytokines, baseline ALBI score, receipt of prior liver directed therapies, and additional dose metrics (DC700cc) as covariates.

Model	Covariate	Coefficient	95% CI LB	95% CI UB	p-value
1	DC700cc (Gy)	0.002	-0.001	0.005	0.286
	Log(sTNFR1)	0.645	0.112	1.178	0.024
	Baseline ALBI Score	-0.192	-0.616	0.231	0.380
	Prior Liver Directed Therapy	0.001	-0.346	0.347	0.998
2	DC700cc (Gy)	0.003	-0.0004	0.005	0.095
	Log(HGF)	0.776	0.340	1.211	0.002
	Baseline ALBI Score	-0.187	-0.559	0.184	0.331
	Prior Liver Directed Therapy	0.136	-0.200	0.471	0.434

Supplemental Table 4. Correlation (ρ) matrix for cytokines.

	HGF	TNFR1
HGF	1.00	0.50 (p=0.001)
sTNFR1	0.50	1.00

Supplemental Table 5. Multivariable model for ΔALBI with multiple cytokines.

Covariate	Coefficient	95% CI LB	95% CI UB	p-value
Log(HGF)	0.488	0.042	0.933	0.040
Log(sTNFR1)	0.177	-0.329	0.683	0.498

Supplemental Table 6. Univariate Cox proportional-hazards model results with dose metrics as covariates for OS. All doses are measured in Gy.

Model	Covariate	HR	95% CI LB	95% CI UB	p-value	c-index
1	MLD	0.99	0.98	1.01	0.403	0.58
2	BED	0.99	0.99	1.00	0.132	0.62
3	EQD2	0.99	0.99	1.00	0.132	0.62
4	DC10	0.98	0.93	1.03	0.381	0.55
5	DC30	0.99	0.97	1.01	0.435	0.54
6	DC90	0.99	0.99	1.00	0.383	0.55
7	DC700cc	0.99	0.99	1.01	0.673	0.55
8	BEDC10	0.99	0.95	1.02	0.393	0.55
9	BEDC30	0.99	0.99	1.01	0.415	0.54
10	BEDC90	0.99	0.99	1.00	0.192	0.55
11	BEDC700cc	0.99	0.99	1.00	0.710	0.55

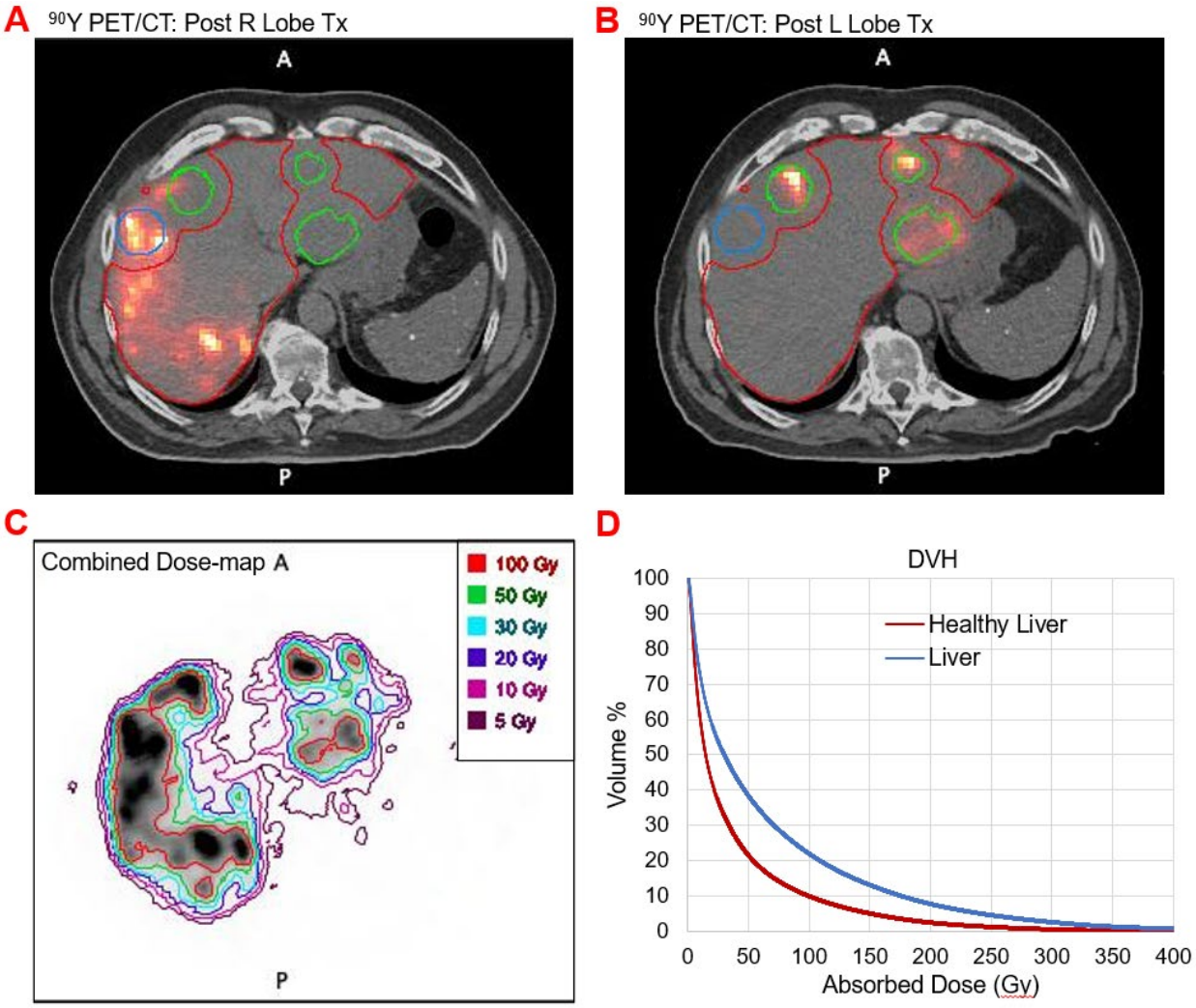

Supplemental Figure 1. Example images for a patient who had two ^{90}Y treatments. A) ^{90}Y PET/CT for a 2.2 GBq treatment to R Lobe and B) ^{90}Y PET/CT for a 0.7 GBq treatment to L Lobe 5 weeks later, co-registered to A. The lesion contours corresponding to the R and L lobe treatments are indicated in blue and green respectively and the non-tumoral liver is indicated in red. C) Dose map and D) DVHs from the two treatments with combined mean absorbed dose to heathy liver of 37 Gy and DC90 100 Gy.

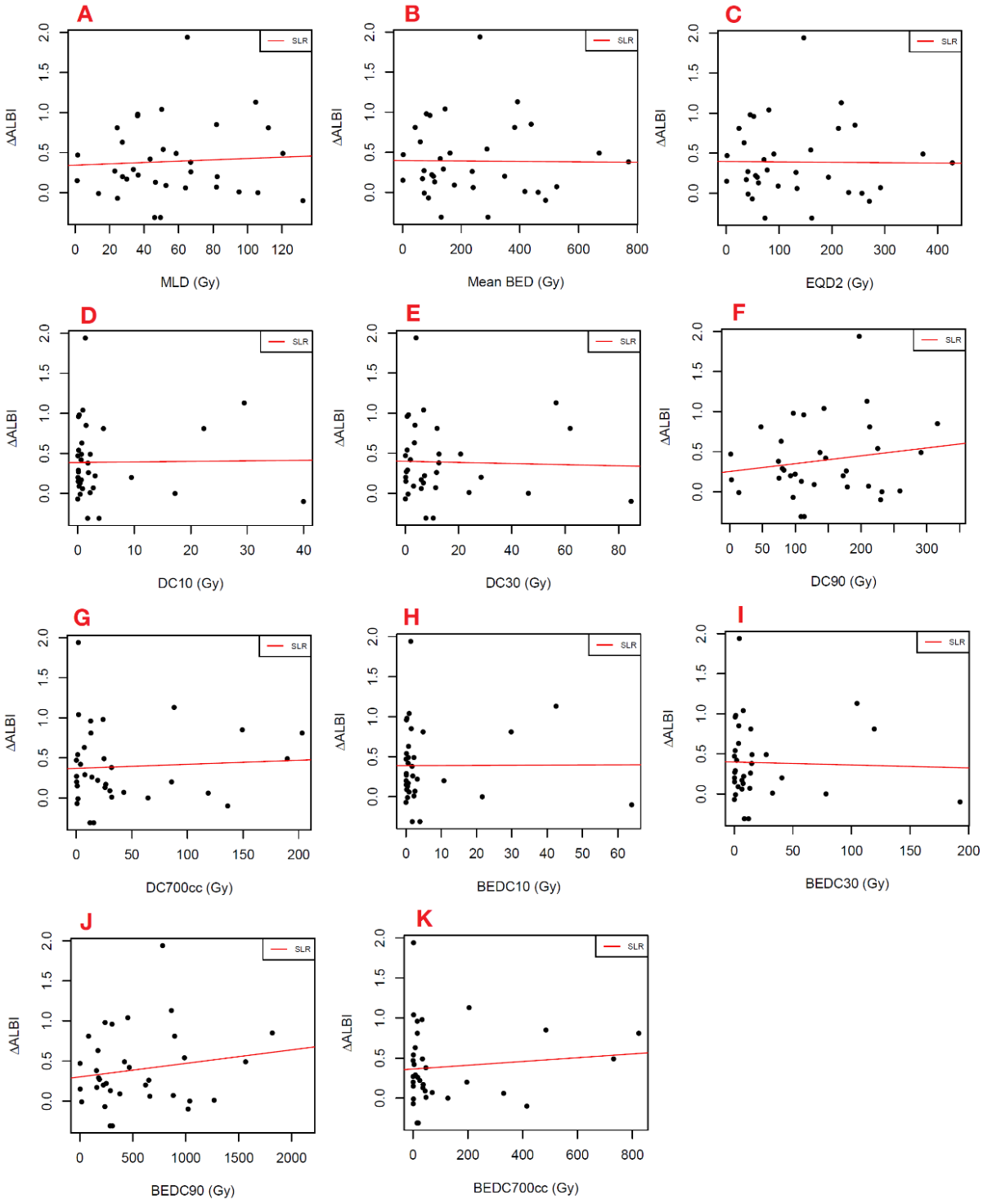

Supplemental Figure 2. Scatterplots of dose metrics (A) MLD, (B) BED, (C) EQD2, (D) DC10, (E) DC30, (F) DC90, (G) DC700cc, (H) BEDC10, (I) BEDC30, (J) BEDC90, and (K) BEDC700cc vs. change in ALBI. Solid red line represents simple linear fit.